Desalination and Water Treatment
www.deswater.com
doi: 10.1080/19443994.2015.1049405

57 (2016) 9009–9017
April

Taylor & Francis
Taylor & Francis Group

An optimal design approach of gas hydrate and reverse osmosis hybrid system for seawater desalination

Hongju Lee[a], Hyunwook Ryu[a], Jun-Heok Lim[b], Jong-Oh Kim[c], Ju Dong Lee[d], Suhan Kim[a,*]

[a]*Department of Civil Engineering, Pukyong National University, 45 Yongso-ro, Nam-gu, Busan 608-737, Korea, Tel. +82 51 629 6065; Fax: +82 51 629 6063; email: suhankim@pknu.ac.kr (S. Kim)*
[b]*Department of Chemical Engineering, Pukyong National University, 365 Sinseon-ro, Nam-gu, Busan 609-739, Korea*
[c]*Department of Civil and Environmental Engineering, Hanyang University, 222 Wangsimni-ro, Seongdong-gu, Seoul 133-791, Korea*
[d]*Offshore Plant Resources R&D Center, Korea Institute of Industrial Technology, 1274 Jisa-dong, Gangseo-gu, Busan 618-230, Republic of Korea*

Received 4 February 2015; Accepted 15 April 2015

ABSTRACT

Gas hydrate (GH) desalination process is based on a liquid (salty water) to solid (GH) phase change coupled with a physical process to separate the GHs from the remaining salty water. However, GH process exhibits less than 90% of salt rejection, so reverse osmosis (RO) process is needed to finally meet the desalinated product water quality. In order to increase the total recovery of the GH and RO hybrid system, the concentrate of the RO process should return to the feed stream of the GH process. In this work, RO simulation was carried out to find an optimal RO recovery with which the energy consumption of RO was minimized. The optimal RO recovery values for GH processes with salt rejection of 78, 84, and 90% were 0.6, 0.8, and 0.8, respectively. The minimal total energy consumption appears at higher RO recovery rates than the optimal values to minimize the RO energy consumption because the portion of the GH energy consumption is inversely proportional to the RO recovery. The simulation also reveals that the maximum allowable energy consumption of GH process is 1.4 kWh/m^3 (with GH salt rejection of 78%) to overcome seawater RO process with energy recovery device, and it can be increased up to 1.9 kWh/m^3 when GH salt rejection increases up to 90%.

Keywords: Gas hydrate; Reverse osmosis; Seawater desalination; Energy consumption

1. Introduction

Due to worldwide water shortage problems, seawater has become an important water source. There are two main seawater desalination methods; one is distillation method such as multi-stage flash and multi-effect distillation, and the other is membrane-based method such as seawater reverse osmosis (SWRO) process. These main desalination methods have been improved to reduce the energy consumption, but the minimum energy consumption is still limited to a range

*Corresponding author.

Presented at IWA Regional Conference on Water Reuse and Energy 2014, 21–24 October 2014, Daegu, Korea

of 3–5 kWh/m^3 (energy consumption in kWh per unit fresh water production in cubic meters) [1,2].

Introduction of novel unit desalination processes such as forward osmosis (FO) and membrane distillation (MD), is expected to break through the limitation of energy consumption. FO and MD are still being investigated through laboratory and pilot tests [3,4]. Gas hydrate (GH)-based desalination process could be one of the novel unit desalination processes and the potential application of GH process was introduced by Park et al. [5], which reported that 72–80% of cations (K^+, Na^+, Mg^{2+}, B^{3+}, and Ca^{2+}) were removed by a single-stage hydrate process using carbon dioxide gas [5].

GHs are nonstoichiometric crystalline inclusion compounds formed by water and a number of gas molecules [6]. Seawater GH without salt compounds is produced in a low temperature and a high pressure condition and they are separated from the remaining liquid phase (concentrated seawater, or salty water). Finally, the separated GHs are dissociated into former gas and pure water for seawater desalination in a high temperature and a low pressure condition. The dissociated gas is reused to produce GHs. Fig. 1 shows the concept of seawater desalination by GH process.

As reported in several literatures [7–10], the limitation of the current GH-based desalination is poor product water quality (i.e. high salt concentration of the desalinated product). The GH product water contains some amounts of ions because it is very difficult to obtain GH slurries free of salty water (concentrated seawater). Further improvement in purity could be accomplished by washing the GH slurries with water or squeezing the GH slurries [5].

The salt rejection by the GH process ranged from 60.5 to 93% according to the literature [5,11,12]. The hydraulic pressure to produce GHs, the selection of gas (e.g. carbon dioxide, cyclopentane, propane, and so on), and washing efficiency determines the GH salt rejection. The energy consumption per unit production by the GH process ranged from 1.58 to 47.9 kWh/m^3 according to the literature [13,14]. The temperature of seawater, the hydraulic pressure to produce GHs, and the selection of gas are dominant factors to determine the GH energy consumption.

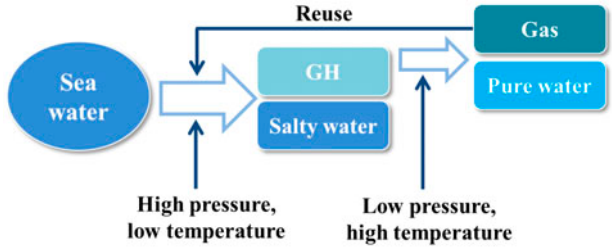

Fig. 1. The concept of GH-based seawater desalination process.

The final goal of the GH-based seawater desalination is, of course, to obtain fresh water from a single-stage hydrate process. However, it is very challenging to reach the final goal so far because of the reason discussed above. Therefore, another desalination process as a post-treatment for the GH process should be introduced to make fresh water. In this study, reverse osmosis (RO) process was selected as the post-treatment following the GH process. The role of RO is the production of fresh water using the GH product to meet the standards for total dissolved solids (TDS) and boron concentration, which is very important design parameter for seawater RO (SWRO) system because boron removal by SWRO membrane is not sufficient to meet the drinking water standards [15]. In the point of view of the RO process, the GH process is one of pretreatment options to decrease salinity of seawater, which is different from the conventional pretreatment technologies including coagulation, adsorption, peroxidation, and prefiltration [16]. By decreasing feed water salinity, the energy consumption of the RO process is expected to be decreased. The objectives of this work are (1) to find the optimal RO recovery to minimize the RO energy consumption and the total energy consumption of the GH and RO hybrid system and (2) to find the maximum allowable GH energy consumption for the hybrid system to have a competitive advantage over the conventional SWRO system.

2. Methods

2.1. Mass balance in the GH and RO hybrid process

Fig. 2 describes the mass balance in the GH and RO hybrid process. In order to increase the total recovery of the GH and RO hybrid system, the concentrate of the RO process should return to the feed stream of the GH process. The GH product TDS concentration ($C_{p,GH}$) can be expressed as:

$$C_{p,GH} = (1 - R_{GH})\, C_{f,GH} \quad (1)$$

where R_{GH} is salt rejection of the GH process and $C_{f,GH}$ is the GH feed TDS concentration. The RO concentrate TDS concentration ($C_{c,RO}$) can be depicted using the GH salt rejection (R_{GH}) and RO recovery (r_{RO}):

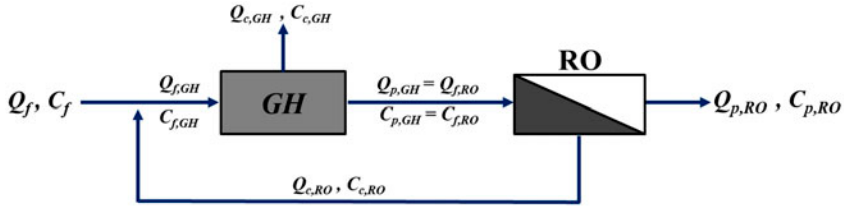

Fig. 2. The mass balance of the GH and RO hybrid process.

$$C_{c,RO} = \frac{C_{p,GH}}{1 - r_{RO}} = \left(\frac{1 - R_{GH}}{1 - r_{RO}}\right) C_{f,GH} \quad (2)$$

The GH feed water consists of seawater and the RO concentrate such as:

$$(Q_f + Q_{c,RO})C_{f,GH} = Q_f C_f + Q_{c,RO} C_{c,RO} \quad (3)$$

where Q_f and C_f is the flow rate and TDS concentration of the feed (seawater) of the hybrid system, and $Q_{c,RO}$ is the RO concentrate flow rate. Using Eqs. (1)–(3), the feed flow rate (Q_f) and the GH feed concentration ($C_{f,GH}$) can be obtained as:

$$C_{f,GH} = \frac{C_f \cdot Q_f}{Q_f + Q_{c,RO} \cdot \left(\frac{R_{GH} - r_{RO}}{1 - r_{RO}}\right)} \quad (4)$$

where r_{GH} is the GH recovery and $Q_{c,RO}$ is the RO concentrate flow rate expressed as:

$$Q_{c,RO} = \frac{1}{r_{RO}} Q_{p,RO} - Q_{p,RO} = \left(\frac{1}{r_{RO}} - 1\right) Q_{p,RO} \quad (5)$$

The input and output flow rates for the total system should be balanced as follows:

$$\begin{aligned} Q_f = Q_{p,RO} + Q_{c,GH} &= Q_{p,RO} + Q_{f,GH} - Q_{p,GH} \\ &= \left[1 + \frac{1}{r_{RO}}\left(\frac{1}{r_{GH}} - 1\right)\right] Q_{p,RO} \end{aligned} \quad (6)$$

where $Q_{p,RO}$ is the RO product flow rate (i.e. the final product of the hybrid system), $Q_{c,GH}$ is the GH concentrate flow rate, $Q_{f,GH}$ and $Q_{p,GH}$ are the GH feed and product flow rates, respectively, and r_{GH} is the GH recovery. $Q_{p,GH}$ and $Q_{f,GH}$ are expressed as:

$$Q_{p,GH} = Q_{f,RO} = \frac{1}{r_{RO}} Q_{p,RO} \quad (7)$$

$$Q_{f,GH} = \frac{1}{r_{GH}} Q_{p,GH} = \frac{1}{r_{RO} r_{GH}} Q_{p,RO} \quad (8)$$

Once the target production rate ($Q_{p,RO}$), feed water condition (Q_f and C_f), and design parameters (R_{GH}, r_{GH}, and r_{RO}) are set, all the related flow rates and concentrates can be obtained using the mass balance as shown in Eqs. (1)–(8).

2.2. The RO feed water quality

As shown in Fig. 2 and Eq. (7), the GH product water is the same as the RO feed water. The GH feed water TDS concentration ($C_{f,GH}$) is obtained from Eq. (4) using known parameters such as the target production rate ($Q_{p,RO}$), feed water condition (Q_f and C_f), and design parameters (R_{GH}, r_{GH}, and r_{RO}). The TDS and ion species concentrations in seawater were obtained from the literature [17]. The ion species considered in this study were Ca^{2+}, Mg^{2+}, Na^+, K^+, Ba^{2+}, Sr^{2+}, Fe^{3+}, Mn^{2+}, Si^{4+}, Cl^-, SO_4^{2-}, F^-, Br^-, NO_3^-, HCO_3^-, and B^{3+}, which are important ions to design RO process [17]. The ion concentration in GH feed were calculated by multiplying the ratio of $C_{f,GH}$ to C_f (i.e. $C_{f,GH}/C_f$) and ion concentration in seawater.

The GH product water quality (i.e. the RO feed water quality) was ion removal rate by the GH process listed in Table 1. The TDS and ion removal rate was taken from the literature [5], where the TDS removal rate was 78% and the ion removal rates of K^+, Na^+, Mg^{2+}, B^{3+}, and Ca^{2+} are 80.4, 78.7, 76.6, 73.3, and 72.0%, respectively. Other GH salt rejection rates such as 84 and 90% were also considered (Table 1) to investigate the effect of the salt rejection rate of the GH process on the product water quality.

2.3. The RO simulation and energy consumption calculation

The RO simulation was carried out using a commercial RO design (simulation) software, CSMPRO by

Table 1
Ion concentrations in seawater and removal rate by the GH process

Ion	Concentration (mg/l) Seawater	TDS rejection rate by GH process (%) 78	84	90
Ca	410	72.0	77.5	83.1
Mg	1,310	76.6	82.5	88.4
Na	10,900	78.7	84.8	90.8
K	390	80.4	86.6	92.8
Ba	0.05	78.0	84.0	90.0
Sr	13.0	78.0	84.0	90.0
Fe	0.02	76.6	82.5	88.4
Mn	0.01	78.0	84.0	90.0
Si	4.0	73.3	78.9	84.6
Cl	19,700	78.0	84.0	90.0
SO_4	2,740	78.0	84.0	90.0
F	1.4	78.0	84.0	90.0
Br	65.0	78.0	84.0	90.0
NO_3	0.7	78.0	84.0	90.0
HCO_3	152	78.0	84.0	90.0
B	5.0	73.3	78.9	84.6
TDS	35,691	78	84	90

Toray Chemical Korea [18]. The input data for the simulation are feed water quality (i.e. ion concentrations, pH, and so on), product flow rate, permeate flux, recovery rate, RO element type, number of elements per pressure vessel (PV), and the PV arrangements. In this study, we selected RE8040-BN for a brackish RO (BWRO) element type and RE8040-SHN for a SWRO element type, which are provided by Toray Chemical Korea [18]. The product flow rate and permeate flux were 1,000 m^3/d and 17 l/m^2 h, respectively. The tested RO recovery rates were in a range of 0.50 to 0.90, and the GH recovery rate was assumed to be 0.50. The feed water temperature was 10°C to simulate low temperature of the GH product.

The output data of the RO process simulation using CSMPRO are the product water quality and the RO feed pressure. The TDS and the boron concentrations obtained from the simulation were controlled to be smaller than 500 and 1 mg/l, respectively, which meet the Korean drinking water standards. The simulated pressure and flow rates of the installed pumps were used to calculate the energy consumption per unit production (E_{RO}, kWh/m^3) using [19]:

$$E_{RO}(kWh/m^3) = \frac{\text{Work done by pumps}}{\eta \times \text{Daily production}} = \frac{Q_{HP}P_{HP} + Q_{BP1}P_{BP1} + Q_{BP2}P_{BP2}}{36\eta Q_{p,RO}} \quad (9)$$

where η, $Q_{HP}P_{HP}$, $Q_{BP1}P_{BP1}$, and $Q_{BP2}P_{BP2}$ are pump efficiency (assumed to be 0.9 in this work), the multiplication between high-pressure pump (HP) flow rate (m^3/d) and pressure (bars), the multiplication between flow rate (m^3/d) and pressure (bars) of the booster pump between the first and second stage (BP1), and the multiplication between flow rate (m^3/d) and pressure (bars) of the booster pump between the second and third stage (BP2), respectively.

3. Results and discussion

3.1. Summary of RO simulation results

Table 2 shows that summary of RO process simulation results including concentrations, flow rates, and PV array. The GH feed TDS ($C_{f,GH}$) decreases at higher GH salt rejections (R_{GH}) because the GH product enters RO process and the RO concentrate returns to the upstream of the GH process with seawater. When the RO recovery (r_{RO}) increases, all the concentrations ($C_{f,GH}$, $C_{p,GH}$, and $C_{c,RO}$) increase because more concentrated salty water due to the higher recovery returns to the GH process, which is a disadvantage of the high RO recovery. The benefit of increasing the RO recovery is to decrease feed flow rates (Q_f, $Q_{f,GH}$, and $Q_{f,RO}$ (=$Q_{p,GH}$)). The number of PVs and elements per each PV are 45 and 8, respectively. According to the guideline of the RO membrane manufacturer [18], the RO element recovery and flux (r_E and J_E) and the feed and concentrate flow rate per element ($Q_{f,E}$ and $Q_{c,E}$) are limited as follows:

$$r_E \le 0.20 \quad (10a)$$

$$J_E \le 39.05\,\text{LMH} \quad (10b)$$

$$Q_{f,RO} \le 396.24\,m^3/d \quad (10c)$$

$$Q_{c,RO} \ge 65.40\,m^3/d \quad (10d)$$

When the RO recovery is high, the limitations in Eq. (10) may not be satisfied with a single-stage design, which is the reason why multi-stage PV array (Fig. 3) is adopted in the RO recovery higher than 60% in Table 2.

Table 3 shows that summary of RO process simulation results including the final product water quality and pump data. The TDS and boron concentrations of the product were controlled to be smaller than 500 and 1 mg/l, respectively, which is the reason why SWRO elements are applied to some process

Table 2
Summary of RO simulation results: concentrations, flow rates, and RO array

r_{RO}	R_{GH}	$C_{f,GH}$ (mg/l)	$C_{p,GH}$ (mg/l)	$C_{c,RO}$ (mg/l)	PV array[a]	Q_f (m^3/d)	$Q_{f,GH}$ (m^3/d)	$Q_{p,GH}$ (m^3/d)	$Q_{c,GH}$ (m^3/d)	$Q_{c,RO}$ (m^3/d)
0.50	0.78	30,080	6,617	13,235	45:0:0	15,000	20,000	10,000	10,000	5,000
	0.84	29,099	4,655	9,311	45:0:0					
	0.90	28,180	2,818	5,636	45:0:0					
0.55	0.78	31,083	6,838	15,196	45:0:0	14,090	18,181	9,090	9,090	4,090
	0.84	30,069	4,811	10,691	45:0:0					
	0.90	29,120	2,912	6,471	45:0:0					
0.60	0.78	32,086	7,058	17,647	45:0:0	13,333	16,666	8,333	8,333	3,333
	0.84	31,039	4,966	12,415	45:0:0					
	0.90	30,059	3,005	7,514	45:0:0					
0.65	0.78	33,088	7,279	20,798	30:15:0	12,692	15,384	7,692	7,692	2,692
	0.84	32,009	5,121	14,633	30:15:0					
	0.90	30,998	3,099	8,856	45:0:0					
0.70	0.78	34,091	7,500	25,000	30:15:0	12,142	14,285	7,142	7,142	2,142
	0.84	32,979	5,276	17,589	30:15:0					
	0.90	31,938	3,193	10,646	45:0:0					
0.75	0.78	35,094	7,720	30,882	30:15:0	11,666	13,333	6,666	6,666	1,666
	0.84	33,949	5,431	21,727	30:15:0					
	0.90	32,877	3,287	13,151	30:15:0					
0.80	0.78	36,096	7,941	39,706	25:15:5	11,250	12,500	6,250	6,250	1,250
	0.84	34,919	5,587	27,935	30:15:0					
	0.90	33,817	3,381	16,908	30:15:0					
0.85	0.78	37,099	8,161	54,412	25:15:5	10,882	11,764	5,882	5,882	882
	0.84	35,889	5,742	38,282	21:13:11					
	0.90	34,756	3,475	23,170	28:12:5					
0.90	0.78	38,102	8,382	83,824	25:12:8	10,555	11,111	5,555	5,555	555
	0.84	36,859	5,897	58,975	23:14:8					
	0.90	35,695	3,569	35,695	24:13:8					

[a]45:0:0 (BWRO), 30:15:0 (BWRO:BWRO), 25:15:5 (BWRO:SWRO:SWRO), 25:12:8 (SWRO:SWRO:SWRO), 21:13:11 (BWRO:BWRO:BWRO), 23:14:8 (BWRO:SWRO:SWRO), 28:12:5 (BWRO:BWRO:BWRO), 24:13:8 (BWRO:BWRO:BWRO).

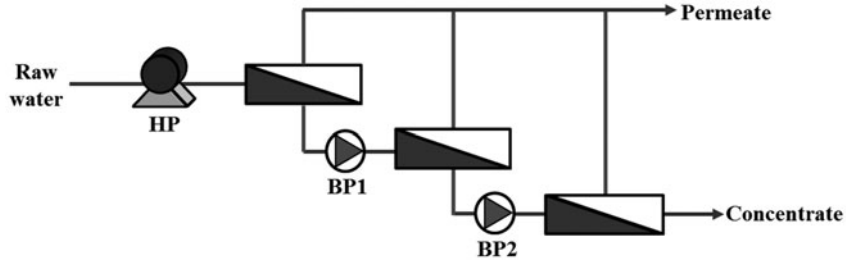

Fig. 3. The schematic of multi-stage RO process to achieve high recovery (HP: high pressure pump, BP: booster pump).

design conditions as shown in Table 2. The pump pressure (P_{HP}) increases at higher RO recovery rates (r_{RO}) and lower GH salt rejections (R_{GH}) due to the increase in osmotic pressure by increased RO feed and concentrate TDS concentrations ($C_{f,RO}$ (=$C_{p,GH}$) and $C_{c,RO}$) as shown in Table 2.

3.2. Effect of RO recovery on RO energy consumption

The RO energy consumption decreases as feed flow rate and feed pressure decrease. Since feed flow rate decreases and feed pressure increases at higher RO recovery rates as shown in Tables 2 and 3, there

Table 3
Summary of RO simulation results: the product water quality and pump data

		Product water quality		HP		BP1		BP2	
r_{RO}	R_{GH}	TDS (mg/l)	Boron (mg/l)	P_{HP} (bar)	Q_{HP} (m^3/d)	P_{BP1} (bar)	Q_{BP1} (m^3/d)	P_{BP2} (bar)	Q_{BP2} (m^3/d)
0.50	0.78	54.9	0.75	19.5	10,000	0	0	0	0
	0.84	38.5	0.49	17.0	10,000	0	0	0	0
	0.90	22.8	0.27	14.5	10,000	0	0	0	0
0.55	0.78	60.9	0.84	19.9	9,090	0	0	0	0
	0.84	42.1	0.55	17.1	9,090	0	0	0	0
	0.90	25.2	0.31	14.6	9,090	0	0	0	0
0.60	0.78	68.2	0.94	20.4	8,333	0	0	0	0
	0.84	46.9	0.62	17.5	8,333	0	0	0	0
	0.90	27.6	0.35	14.7	8,333	0	0	0	0
0.65	0.78	74.8	0.99	22.3	7,692	1	3,702	0	0
	0.84	53.0	0.67	19.5	7,692	0	0	0	0
	0.90	30.6	0.40	14.9	7,692	0	0	0	0
0.70	0.78	74.6	0.99	19.1	7,142	10	4,071	0	0
	0.84	58.4	0.73	19.7	7,142	0	0	0	0
	0.90	35.3	0.47	15.3	7,142	0	0	0	0
0.75	0.78	76.1	0.98	16.7	6,666	17	4,270	0	0
	0.84	68.7	0.84	20.6	6,666	0	0	0	0
	0.90	38.8	0.47	16.7	6,666	0	0	0	0
0.80	0.78	94.9	0.99	28.4	6,250	8	1,898	0	0
	0.84	84.0	0.96	21.7	6,250	0	0	0	0
	0.90	46.3	0.56	17.3	6,250	0	0	0	0
0.85	0.78	106.5	0.99	27.4	5,882	18	1,848	0	0
	0.84	89.4	0.99	20.1	5,882	5	3,075	7	1,616
	0.90	46.1	0.58	14.1	5,882	10	3,024	0	0
0.90	0.78	95.5	0.47	48.1	5,555	9	2,142	0	0
	0.84	83.3	0.72	24	5,556	15	1,788	10	931
	0.90	69.5	0.73	17.4	5,556	5	2,363	5	908

must exist an optimal RO recovery rate to minimize the RO energy consumption. Fig. 4 shows the RO energy consumption as a function of RO recovery rate. The minimal RO energy consumption appears at 0.60 (R_{GH} = 78%), 0.80 (R_{GH} = 84%), and 0.80 (R_{GH} = 90%) of the RO recovery. The sudden increase in the energy consumption is observed in 0.90 of the RO recovery at R_{GH} = 78% because SWRO elements are adopted for all PVs to control boron concentration smaller than 1 mg/l as shown in Tables 2 and 3. As the salt rejection of GH process (R_{GH}) increases from 78 to 90%, the minimal RO energy consumption decreases from 0.94 to 0.60 kWh/m^3.

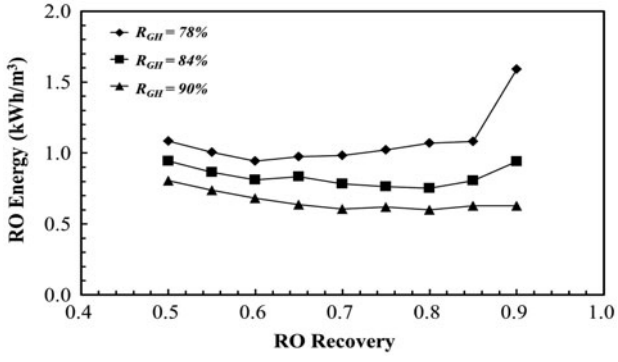

Fig. 4. Effect of RO recovery on the RO energy consumption.

3.3. Effect of RO recovery on the total energy consumption

Fig. 5 shows total energy consumption as a function of the RO recovery when the GH energy consumption (E_{GH}, kWh/m^3) is assumed to be 1.5, 2.0, and 2.5 kWh/m^3, respectively. The total energy consumption (E_T, kWh/m^3) can be calculated using:

$$E_T = \frac{E_{GH}Q_{p,GH} + E_{RO}Q_{p,RO}}{Q_{p,RO}} = E_{GH}/r_{RO} + E_{RO} \quad (11)$$

Thus, the portion of the GH energy consumption (E_{GH}/r_{RO}) in the total energy consumption should

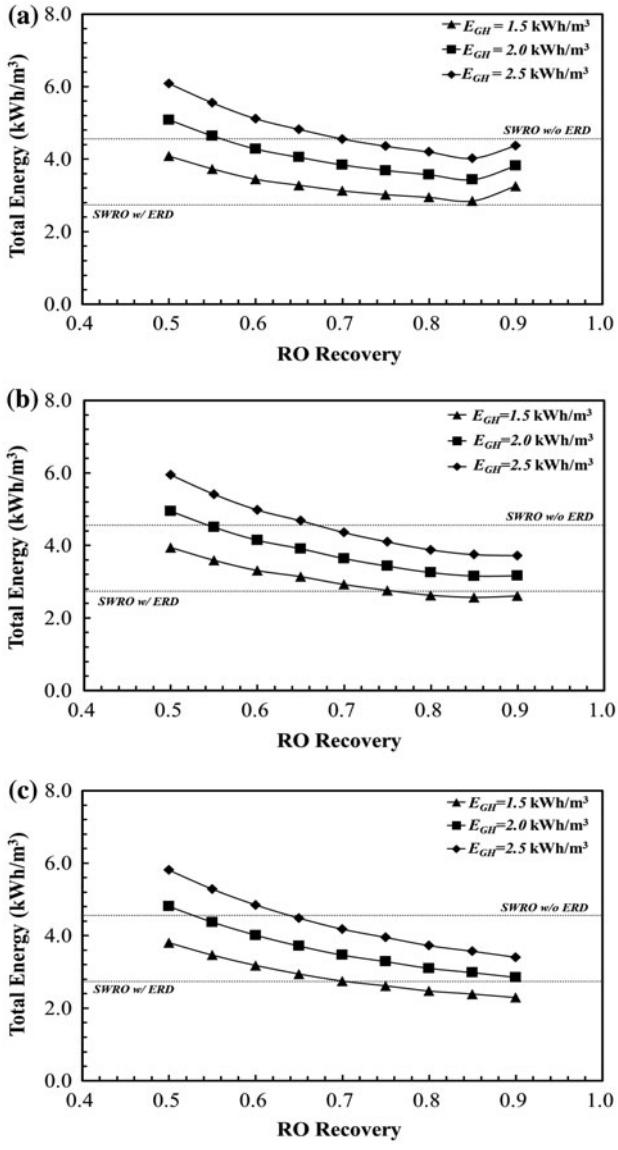

Fig. 5. Effect of RO recovery of the GH process on total energy consumption at (a) R_{GH} = 78%, (b) R_{GH} = 84% and (c) R_{GH} = 90%.

decrease as the RO recovery increases. This is the reason why the minimal total energy consumption appears at higher RO recovery rates (Fig. 5) than the optimal values to minimize the RO energy consumption (Fig. 4). When the GH salt rejection is higher than 84%, the portion of the GH energy consumption in the total energy consumption becomes dominant and the minimal total energy consumptions appears at the highest RO recovery rates to minimize the GH product flow rate (i.e. the GH product flow rate is the same as the RO feed flow rate.) as shown in Fig. 5(b) and (c).

3.4. Effect of the GH process performance on the total energy consumption

The total energy consumption can be compared to a reference value. In this work, two reference values (i.e. the energy consumption values in conventional SWRO system with or without energy recovery device (ERD)) were obtained by the simulation procedure described in the Section 2.3. In the simulation of the conventional SWRO system, most of input conditions are the same as those of the RO simulation for the GH and RO hybrid system, but feed water and recovery rate are different. Seawater was used as feed water and the recovery rate was assumed to be 0.50 in the conventional SWRO simulation. The simulation revealed that the feed pressure was 73.9 bars, which results in 4.56 kWh/m^3 of the energy consumption in conventional SWRO system without ERD calculated using Eq. (9). Energy saving by ERD (E_{ERD}) can be calculated using [19]

$$E_{ERD} = \frac{\eta_{ERD}\, Q_{c,RO}\, P_{c,RO}}{36 Q_{p,RO}} \tag{12}$$

where $Q_{c,RO}$ (m^3/d) is RO concentrate flow rate ($Q_{c,RO} = Q_d$); $P_{c,RO}$(bar) is RO concentrate pressure; and the ERD efficiency (η_{ERD}) was assumed to be 0.9. Energy saving by ERD was determined to be 1.82 kWh/m^3, which results in 2.74 kWh/m^3 of the energy consumption in conventional SWRO system with ERD.

The two reference values, 4.56 and 2.74 kWh/m^3 appears in Fig. 5 to be compared with the total energy consumption of the RO and GH hybrid system. As a result, the RO and GH hybrid system with optimized RO recovery is competitive while the minimal total energy consumption is lower than that in the conventional SWRO system without ERD. However, the conventional SWRO system is more energy efficient than the hybrid system in the most design cases if ERD is adapted to the SWRO system as shown in Fig. 5. The two cases when the hybrid system has a competitive advantage over the SWRO system with ERD appears at 1.5 kWh/m^3 of the GH energy consumption when the GH salt rejection is 84 and 90% (Fig. 5(b) and (c)).

Fig. 6 shows the total energy consumption (i.e. the sum of the RO and GH energy consumptions) of the hybrid system as a function of the GH energy consumption. The RO energy consumption was calculated using Eq. (9) with the optimal RO recovery value which makes the total energy consumption minimal at a certain GH energy consumption and GH salt rejection. For example, the optimal RO recovery value is 0.85 at

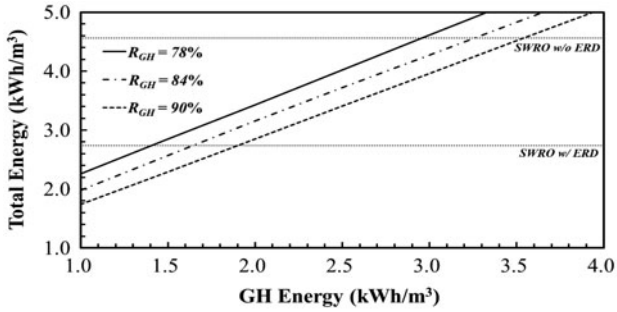

Fig. 6. Effect of the GH energy consumption on the total energy consumption.

1.5 kWh/m^3 of the GH energy consumption and 79% of the GH salt rejection (Fig. 5(a)) and it becomes 0.90 at 2.5 kWh/m^3 of the GH energy consumption and 90% of the GH salt rejection (Fig. 5(c)). As shown in Fig. 6, the total energy consumption decreases at the lower GH energy consumptions and the higher GH salt rejections. The GH energy consumption should be less than 2.9 kWh/m^3 (R_{GH} = 78%), 3.2 kWh/m^3 (R_{GH} = 84%), and 3.5 kWh/m^3 (R_{GH} = 90%) to have a competitive advantage over the SWRO system without ERD, and it should be less than 1.4 kWh/m^3 (R_{GH} = 78%), 1.6 kWh/m^3 (R_{GH} = 84%), and 1.9 kWh/m^3 (R_{GH} = 90%) to compete with the SWRO system with ERD.

4. Conclusions

The GH and RO hybrid system can be one of new promising desalination technologies to decrease the energy consumption. In this system, RO concentrate should return to the GH feed stream and the RO recovery is an important factor to minimize the energy consumption of the hybrid system. The RO simulation reveals that (1) the optimal RO recovery values for GH processes with salt rejection of 78, 84, and 90% were 0.6, 0.8, and 0.8, respectively; (2) the minimal total energy consumption appears at higher RO recovery rates than the optimal values to minimize the RO energy consumption because the portion of the GH energy consumption is inversely proportional to the RO recovery; and (3) the maximum allowable energy consumption of GH process to overcome seawater RO process with ERD is 1.4–1.9 kWh/m^3 according to GH salt rejection. The salt rejection and energy consumption of the GH process are two key parameters to determine the economic value of the GH and RO hybrid system for seawater desalination.

Acknowledgment

This research was a part of the project titled "Development of key technology in seawater desalination using gas hydrate process" funded by Ministry of Oceans and Fishery, Korea.

References

[1] S. Kim, D. Cho, M.S. Lee, B.S. Oh, J.H. Kim, I.S. Kim, SEAHERO R&D program and key strategies for the scale-up of a seawater reverse osmosis (SWRO) system, Desalination 238 (2009) 1–9.
[2] S. Kim, B.S. Oh, M.H. Hwang, S. Hong, J.H. Kim, S. Lee, I.S. Kim, An ambitious step to the future desalination technology: SEAHERO R&D program (2007–2012), Appl. Water Sci. 1 (2011) 11–17.
[3] T.Y. Cath, A.E. Childress, M. Elimelech, Forward osmosis: Principles, applications, and recent developments, J. Membr. Sci. 281 (2006) 70–87.
[4] M. Khayet, T. Matsuura, Membrane Distillation—Principles and Applications, Elsevier, Oxford, 2011.
[5] K.N. Park, S.Y. Hong, J.W. Lee, K.C. Kang, Y.C. Lee, M.G. Ha, J.D. Lee, A new apparatus for seawater desalination by gas hydrate process and removal characteristics of dissolved minerals (Na^+, Mg^{2+}, Ca^{2+}, K^+, B^{3+}), Desalination 274 (2011) 91–96.
[6] E.D. Sloan Jr., Clathrate Hydrates of Natural Gases, second ed., Marcel Dekker, New York, NY, 1998.
[7] R.A. McCormack, R.K. Andersen, Clathrate Desalination Plant Preliminary Research Study, U.S. Department of the Interior, Bureau of Reclamation, 1995.
[8] R.A. McCormack, G.A. Niblock. Build and Operate Clathrate Desalination Pilot Plant U.S. Department of the Interior, Bureau of Reclamation, 1998.
[9] R.A. McCormack, G.A. Niblock, Investigation of High Freezing Temperature, Zero Ozone, and Zero Global Warming Potential, Clathrate Formers for Desalination, U.S. Department of the Interior, Bureau of Reclamation, 2000.
[10] Y.T. Ngan, P. Englezos, Concentration of mechanical pulp mill effluents and NaCl solutions through propane hydrate formation, Ind. Eng. Chem. Res. 35 (1996) 1894–1900.
[11] K.C. Kang, P. Linga, K. Park, S.J. Choi, J.D. Lee, Seawater desalination by gas hydrate process and removal characteristics of dissolved ions (Na^+, K^+, Mg^{2+}, Ca^{2+}, B^{3+}, Cl^-, SO_4^{2-}), Desalination 353 (2014) 84–90.
[12] S. Han, J.Y. Shin, Y.W. Rhee, S.P. Kang, Enhanced efficiency of salt removal from brine for cyclopentane hydrates by washing, centrifuging, and sweating, Desalination 354 (2014) 17–22.
[13] P.G. Youssef, R.K. AL-Dadah, S.M. Mahmoud, Comparative analysis of desalination technologies, Energy Procedia 61 (2014) 2604–2607.
[14] J. Javanmardi, M. Moshfeghian, Energy consumption and economic evaluation of water desalination by hydrate phenomenon, Appl. Therm. Eng. 23 (2003) 845–857.

[15] H.H. Vu, B.Y. Cho, A Study on boron removal by mineral cluster coagulant for seawater desalination application, Environ. Eng. Res. 16(4) (2011) 227–230.
[16] R. Valavala, J. Sohn, J. Han, N. Her, Y. Yoon, Pretreatment in reverse osmosis seawater desalination: A short review, Environ. Eng. Res. 16(4) (2011) 205–212.
[17] Dow liquid separations, Filmtec reverse osmosis membranes technical manual, The Dow Chemical Company Form No. 609-00071-0705, 2005.
[18] CSM webpage. Available from: <http://www.csmfilters.com>.
[19] S.H. Park, B. Park, H.K. Shon, S. Kim, Modeling full-scale osmotic membrane bioreactor systems with high sludge retention and low salt concentration factor for wastewater reclamation, Bioresour. Technol. (2015). doi: 10.1016/j.biortech.2015.03.094.